JOURNAL OF SOLID STATE CHEMISTRY 100, 141–150 (1992)

Raman and Infrared Spectra of Some Chromium Nasicon-Type Materials: Short-Range Disorder Characterization

M. BARJ*

Laboratoire d'Ingéniérie des Matériaux et des Hautes Pressions-L.I.M.H.P (UP CNRS 1311), Université Paris-Nord, Av. J. B. Clément, F-93430 Villetaneuse, France

G. LUCAZEAU

Laboratoire d'Ionique et d'Electrochimie du solide-L.I.E.S, ENSEEG, BP 75, F-38402 Saint Martin d'Hères cedex, France

AND C. DELMAS

Laboratoire de Chimie du Solide du CNRS, Université Bordeaux-I, 351 Cours de la Libération, F-33405 Talence cedex, France

Received November 19, 1991; in revised form March 4, 1992; accepted March 6, 1992

The infrared and Raman spectra of the Nasicon-type chromium systems are found to be very sensitive to the composition and to the nature of the metallic ions. The frequency shift of the infrared active modes involving the metallic ions is correlated to the modification of the crystal field around these ions. The static short-range disorder, particularly characterized from the Raman spectra, is essentially interpreted in terms of Na^+ ion site occupation change vs the composition and the temperature.

1. Introduction

The materials investigated in this paper correspond to $Na_3L_2(PO_4)_3$ with $L = Cr^{3+}$ and Fe^{3+}, and to $Na_{1+x}Zr_{2-x}Cr_x(PO_4)_3$ and $Na_{3+y}Cr_{2-y}Mg_y(PO_4)_3$ solid solutions previously studied by Delmas and co-workers (*4–6*). These compounds belong to the Nasicon (*Na* Super*I*onic *Con*ductor) structural family first studied by H.Y-P. Hong (*1*). The study of the $Na_3L_2(PO_4)_3$ terms is particularly interesting because they present sodium content and vacancy rate "similar" to that of "true" Nasicon $Na_3Zr_2Si_2PO_{12}$. Structural studies on single crystals of these compounds have been performed (*7, 8*) on the monoclinic and rhombohedral crystallographic phases. The order–disorder transitions and the increasing of the conductivity have been correlated to the Na^+ distribution on the available cationic sites. Specific heat

* To whom correspondence should be addressed at Laboratoire PMTM (UP 9001 CNRS), Institut Galilee, Université Paris-Nord, Avenue J. B. Clément, F-93430 Villateneuse, France.

0022-4596/92 $5.00

(C_p) measurements (*9, 14*) on $Na_3Cr_2(PO_4)_3$ and $Na_3Fe_2(PO_4)_3$ have been interpreted in terms of entropy excess associated with a disorder model (*11*) based on the occupation factor variations (*7*). Potential energy calculations (*11*) have shown that relaxation motions such as PO_4 rotations associated with the expansion of the diffusion bottlenecks must be taken into account in the diffusion mechanism. The Neutron scattering experiments (*2, 10*) have not completely allowed the study of the Na^+ cation dynamics in $Na_3Cr_2(PO_4)_3$ for which the observed quasielastic QES component has been attributed essentially to a magnetic scattering of Cr^{3+} ions. However, a localized-jumps model could fit nicely the experimental QES recorded at high temperature and for large scattering vectors (*2*).

The infrared and Raman study presented here is a part of the general vibrational investigations we have initiated on the Nasicon family in order to determine the dynamics of the monovalent mobile cations (*2, 3*). We report in this paper the principle results obtained for different composition of the chromium solid solutions described above. A general band assignment is presented in the case of $Na_3L_2(PO_4)_3$. Then the spectral evolution with the composition and the temperature is discussed in term of static and/or dynamic order–disorder presence. The frequency shift of the mean L–O vibrations is correlated to the L^{3+} crystal field.

2. Experimental

2.1. Synthesis

The powders have been prepared from finely ground stoichiometric mixtures of Na_2CO_3, $(NH_4)_2HPO_4$, and metal oxides (*4–6, 15*). The solid-state reaction temperature depends on the nature of the metal, around 900°C with iron and 1000°C with chromium or zirconium. All the polycrystalline samples have been characterized by X-ray diffraction.

2.2. Spectra

Infrared absorption spectra have been recorded on a Perkin–Elmer 580 spectrometer for the 4000–190 cm^{-1} spectral range and on a Polytec FIR spectrometer for the low-frequency region. The polycrystalline samples were dispersed in KBr, CsI, or polyethylene pressed pellets.

The Raman spectra have been obtained using a Coderg T800 spectrometer equipped with argon or krypton lasers.

3. Structure and Vibrational Selection Rules

As shown in Fig. 1, the Nasicon structure consists of a three-dimensional framework built with PO_4/SiO_4 tetrahedra corner-linked to ZrO_6 and NaO_6 octahedra. Infinite ribbons $(O_3ZrO_3Na(1)O_3ZrO_3)_n$ connected by the tetrahedra are then defined. The structure is described by the rhombohedral $R\bar{3}c$ space group (*12, 13*). When substituting alkali or metallic cations, monoclinic distortion is observed (*1, 7, 8*); the structure is then described by the $C2/c$ space group. In both cases there are two formula units per primitive cell.

For $Na_3L_2(PO_4)_3$, a $C2/c$ monoclinic structure is observed at room temperature (α-phase). The high-temperature β- and γ-phases are rhombohedral. In this last case, the Na^+ ions may occupy two kinds of sites, labeled Na(1) and Na(2), which correspond respectively to the $6b(\bar{3})$ and $18e(2)$ wyckoff positions of the $R\bar{3}c$ space group. This is shown in Fig. 1 for the directions parallel and perpendicular to the hexagonal c-axis. The Na(1) site is fully occupied in $Na\ Zr_2(PO_4)_3$ and partially filled as L^{3+} is substituted for Zr^{4+}. All the Na(1) and Na(2) sites are fully occupied in $Na_4Zr_2(SiO_4)_3$ (*13*) and probably in $Na_4CrMg(PO_4)_3$.

The vibrational modes of the Nasicon lattice can be assigned to PO_4 tetrahedra internal and external modes, and to lattice modes including the motions of the metallic L^{3+}

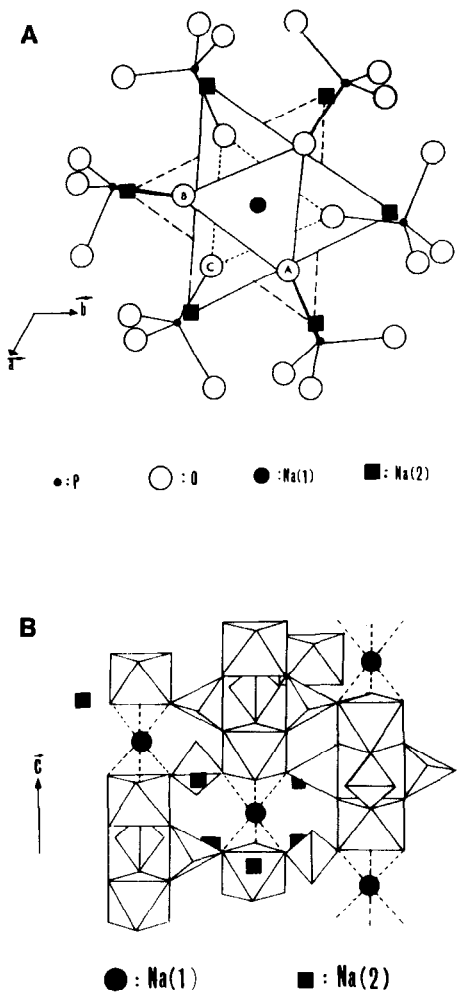

FIG. 1. Projection on the xOy plane (A) and perspective view parallel to the c-axis (B) of the Nasicon-type structure. The six Na(2) sites around an Na(1) site are presented (hexagonal description).

and Na^+ ions in their octahedral cage. The internal modes of the phosphate ions represent the symmetric ν_s(PO) and antisymmetric degenerate ν_d(PO) of phosphorous-nonbridging oxygen stetchings, and the symmetric/antisymmetric degenerate δ_d(OPO) bendings. These modes are usually labeled ν_1, ν_2, ν_3, and ν_4, respectively. The PO_4 external modes correspond to librational and translational motions of these groups.

Applying the usual factor group correlation methods (*2*), the irreductible representations for the monoclinic $C_{2h}(C2/c)$ and rhombohedral $D_{3d}(R\bar{3}c)$ factor groups can be evaluated respectively as follows:

$$\Gamma_1 = 29\,A_g + 31\,B_g + 32\,A_u + 34\,B_u$$

$$\Gamma_2 = 9\,A_{1g} + 11\,A_{2g}^* + 20\,E_g + 10\,A_{1u}^* + 12\,A_{2u} + 22\,E_u.$$

The A_{2g} and A_{1u} are optically inactive. Thus, since acoustic modes ($A_{2u} + E_u$) must be substracted, 29 Raman and 32 IR active modes are expected in the case of a rhombohedral cell. The monoclinic distortion introduces a splitting of P and Na sites. So one expects, for the C_{2h} factor group, 60 Raman and 63 IR modes.

4. General Band Assignments

The infrared and Raman band wavenumbers at 300 K and the corresponding assignments previously proposed for $Na_3Cr_2(PO_4)_3$ and $Na_3Fe_2(PO_4)_3$ (*2*) are given in Table I. The corresponding spectra are given in Figs. 2–3 and Figs. 5–7.

For the iron compound, the number of observed bands agree well with the selection rules predictions for a monoclinic symmetry. This is not the case for $Na_3Cr_2(PO_4)_3$, for which the number of vibrational components (principally Raman) is far from the expected modes for the C_{2h} or D_{3d} factor groups. The reduction of the number of vibrational components and the observation of very broad bands are the indication of an important short-range static disorder (discussed hereafter). The same broad bands were also observed in the Raman polarized spectra of an $Na_3Cr_2(PO_4)_3$ single crystal (*2*).

All the stretching and bending modes of the phosphate groups are located above 390 cm^{-1}, as for Na_3PO_4 (*17*). The assignment of the external modes is more difficult. How-

TABLE I

IR AND RAMAN BAND WAVENUMBERS (cm^{-1}) OF $Na_3L_2(PO_4)_3$. L = Fe, Cr

$Na_3Fe_2P_3O_{12}$		$Na_3Cr_2P_3O_{12}$		Approximate type of motion
Raman	IR	Raman	IR	
1215 w	1215 m	—	—	
—	1180 s	—	1185 m	
1160 w	—	—	1160 vw	
1130 vw	1135 m	1130 sh	1135 vw	
—	1110 sh	—	1120 vw	
—	1095 sh	—	1090 s	$\nu_3(PO_4)$
1060 m	1065 vs	1060 vs	1075 sh	
1045 vs	1045 vs	—	1050 sh	
1034 sh,s	—	1030 sh	—	
1025 sh,s	1026 s	—	—	
1019 sh,s	1020 sh	—	1015 sh	
1015 vs	—	—	1010 sh	
–	1005 sh	—	1005 sh	
973 s	975 vs	990 sh	990 s	
963 m	967 sh	—	975 s	$\nu_1(PO_4)$
—	960 sh	—	—	
—	935 sh	—	930 s	
—	915 sh	—	—	
642 vw	650 sh	—	667 w	
624 w	625 m	630 w	632 m	
597 w	—	595 w	—	
586 w	585 m	—	585 sh	
—	575 m	—	575 m	$\nu_4(PO_4)$
560 w	545 vw	555 w	545 w	
543 w	537 w	—	—	
480 vw	490 sh	—	—	
—	465 sh	—	465 sh	
445 m	440 sh	455 m	450 sh	$\nu_2(PO_4)$
—	398 s	—	405 s	
—	365 sh	—	370 s	Fe and Cr modes
330 w	335 vs	350 m	—	
320 m	—	340 sh	—	
290 w	285 sh	295 m	300 vw	
—	—	270 sh	275 w	
237 m	245 s	—	240 m	
204 sh	—	210 w	—	T′(PO_4) and R′(PO_4)
195 m	—	—	197 w	
172 m	—	175 w	183 w	
147 m	—	140 m	—	
131 m	—	—	—	
—	—	—	115 m	T′(Na1)
82 w	—	—	85 m	
72 w	—	75 m	—	T′ or R′(PO_4)
60 w	—	—	—	
49 w	—	50 m	52 m	T′(Na2)

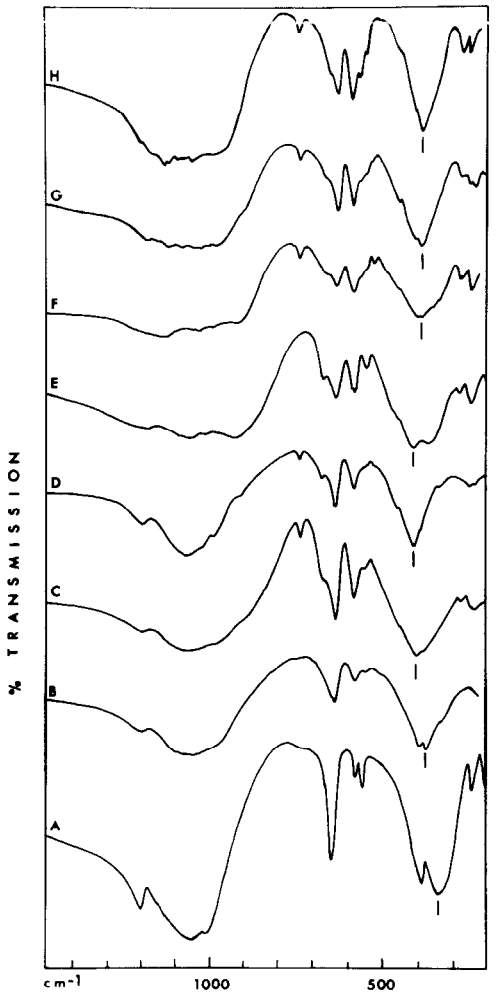

FIG. 2. The infrared absorption spectra (1500–200 cm^{-1}) of: (A) $NaZr_2P_3O_{12}$, (B) $Na_2CrZrP_3O_{12}$, (C) $Na_{2.7}Cr_{1.7}Zr_{0.3}P_3O_{12}$, (D) $Na_{2.9}Cr_{1.9}Zr_{0.1}P_3O_{12}$, (E) $Na_3Cr_2P_3O_{12}$, (F) $Na_{3.4}Cr_{1.6}Mg_{0.4}P_3O_{12}$, (G) $Na_{3.65}Cr_{1.35}Mg_{0.65}P_3O_{12}$, and (H) $Na_4CrMgP_3O_{12}$.

ever, the IR and Raman components located in the 300–120 cm^{-1} seem to be insensitive to the metal substitution (no significant frequency shift) and then could be reasonably attributed to the translational and librational modes of the PO_4 ions.

The 405–370 cm^{-1} infrared doublet and the 340–350 cm^{-1} Raman components of $Na_3Cr_2(PO_4)_3$ are very sensitive to the metal substitution and, thus, could be associated with the CrO_6 motions. Similar frequencies are reported for Cr_2O_3 (*16*). These frequencies shift to 398–335 cm^{-1} (IR) and 330–320 cm^{-1} (Raman) in $Na_3Fe_2(PO_4)_3$. The 405- and 398-cm^{-1} infrared bands are very likely components of the ν_2 symmetric degenerate phosphate bendings.

The low-freqency modes observed around 85 cm^{-1} in the far-infrared spectra are attributed to the Na^+ motions in the Na(1) rhombohedral site for which only an infrared active mode is expected (*2, 3, 18*). The active modes associated with the occupation of the Na(2) site are observed around 50 cm^{-1} both in Raman and FIR spectra. This assignment is based on the frequency shift observed for different monovalent cation compounds and on the appearance of

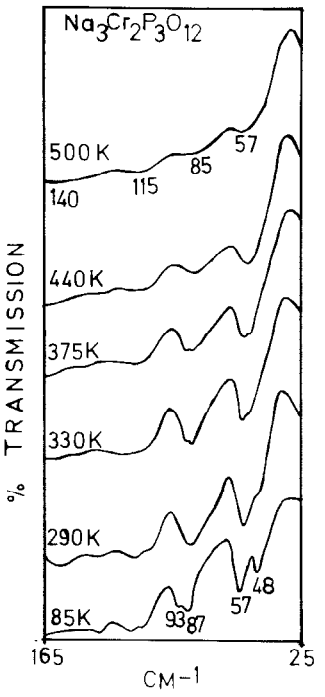

FIG. 3. Far-infrared spectra (165–25 cm^{-1}) of $Na_3Cr_2P_3O_{12}$ between 85 and 500 K.

new bands when the Na(2) site is occupied as in $Na_4Zr_2(SiO_4)_3$ or $Na_3ZrMg(PO_4)_3$ (*17*). All these modes seem to split in the ordered iron compound (monoclinic phase at the ambient temperature) and also for the chromium compound, as shown by the FIR spectra recorded below 300 K (Fig. 3).

5. Vibrational Analysis of the Chromium Solid Solutions

5.1. Discussion of the IR Absorption and Raman Spectra

Figure 2 shows the spectral evolution of the high- and medium-frequency infrared absorption spectra at room temperature of the NaZrCr and NaCrMg solid solutions vs the sodium content. In this region, two significant spectral modifications are observed:

(i) the width of the ν_1–ν_3 broad IR features seems to increase with the filling of the available sodium sites and depends on the chemical nature of the metal. It presents a maximum for $Na_3Cr_2(PO_4)_3$. This very broad absorption feature presents only few well-defined bands. The mean frequency of these bands seems to increase slightly with the sodium content.

(ii) the average frequency of the metal sensitive bands (L^{n+} motions in LO_6) increases significantly from 330 cm^{-1} in $NaZr_2(A)$ to 405 cm^{-1} in $Na_3Cr_2(E)$ and decreases, when Mg^{2+} ions substitute Cr^{3+} ions, to 385 cm^{-1} in $Na_4CrMg(H)$. In spite of the fact that two kinds of LO_6 octahedra, $(Zr, Cr)O_6$ and $(Cr, Mg)O_6$, exist, only an average frequency is observed. The continuous frequency shift is not exclusively due to the L metal mass variation but rather related to the mean L–O bonding. When the average metal mass decreases, as in Na_4CrMg, a frequency increase is usually expected. Instead of that, a decrease of the mean frequency is observed. It is probably due to coupling with phosphate bending modes in addition to the metal cation effects

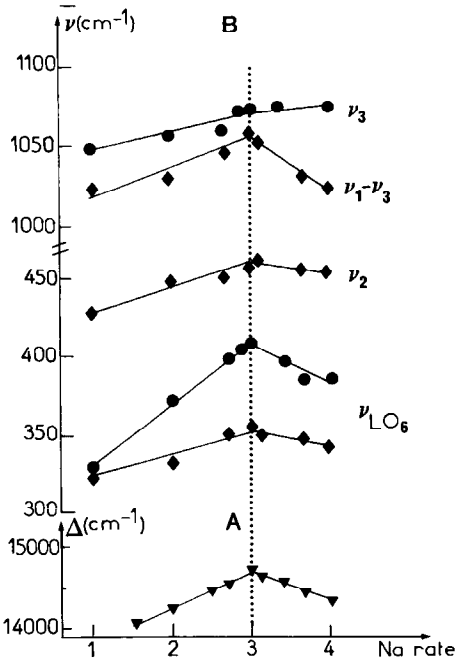

FIG. 4. (A) Crystal field variation (from Ref. (*4*)) and (B) vibrational (IR, Raman) frequency shifts as a function of sodium content for chromium-substituted phases.

such as ionic size and distribution. However, on the basis of the structural studies reported in Ref. (*4*), we consider that the crystal-field effects are strongly involved. This is clearly illustrated in Fig. 4; the mean frequency increases with the crystal field. The highest $\nu(LO_6)$ is observed in Na_3Cr_2, for which the crystal field is maximum (*4*).

The increase of the crystal field is an indication that the covalent character of L–O bonds increases. The increase of d_L–$2p_0$ overlap could be due to a structural rearrangement of the "ribbons" (*4*) associated to an increase of the metal d orbitals size. When Mg ions are introduced in the L-sites, the covalent character is lost and the PO_4 groups recover their ionicity as in orthophosphates such as Na_3PO_4. As a con-

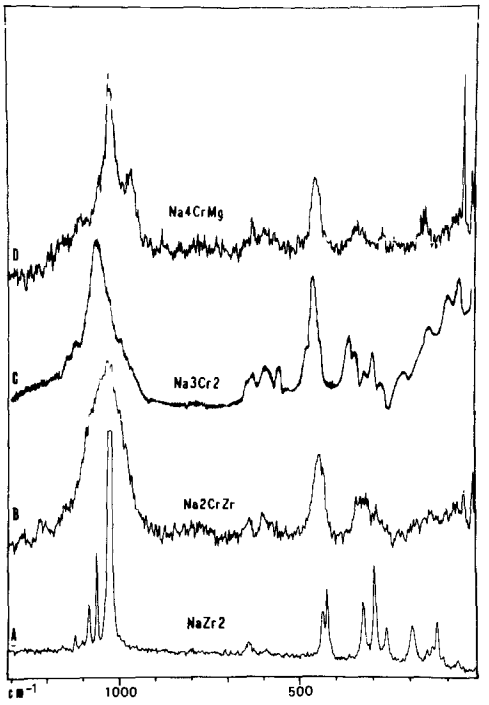

FIG. 5. Raman spectra (10–1300 cm^{-1}) of: (A) $NaZr_2P_3O_{12}$, (B) $Na_2CrZrP_3O_{12}$, (C) $Na_3Cr_2P_3O_{12}$, and (D) $Na_4CrMgP_3O_{12}$.

sequence the corresponding frequencies decrease.

The Raman spectra shown in Fig. 5 exhibit the same trends as the IR spectra. For the *L*-metal-sensitive modes and for the phosphate internal modes, a frequency maximum is also observed around the composition $Na_3Cr_2(PO_4)_3$ corresponding to the highest value of the crystal field. But the most drastic change cooncerns the modification of the number of the Raman components, which is discussed below.

5.2. *Spectral Variations and Disorder*

Evolution with the composition. When the sodium content increases, the width of the Raman components drastically increases. At the same time, the number of the observed bands decreases considerably from $NaZr_2(PO_4)_3$ to $Na_4CrMg(PO_4)_3$ compositions. This is correlated to the establishment of static short-range disorder (SSRD) essentially associated with the partial occupation of the sodium sites. In $NaZr_2$ all the Na(1) rhombohedral sites are occupied, the Na(2) are empty, the Raman spectrum (Fig. 6) presents well-defined components. The width and the number of these components are compatible with an ordered compound. That is also the case when all the Na^+ available sites are occupied as for $Na_4Zr_2(SiO_4)_3$ (*2, 3*) or $Na_4CrMg(PO_4)_3$. However, for this last compound, the broadening of the Raman bands is associated with a SSRD due to the Cr/Mg statistical distribution on the available metallic sites. This is certainly the case in $Na_2CrZr(PO_4)_3$.

In $Na_3Cr_2(PO_4)_3$ the SSRD is associated with the sodium site occupation (*9, 15*). The

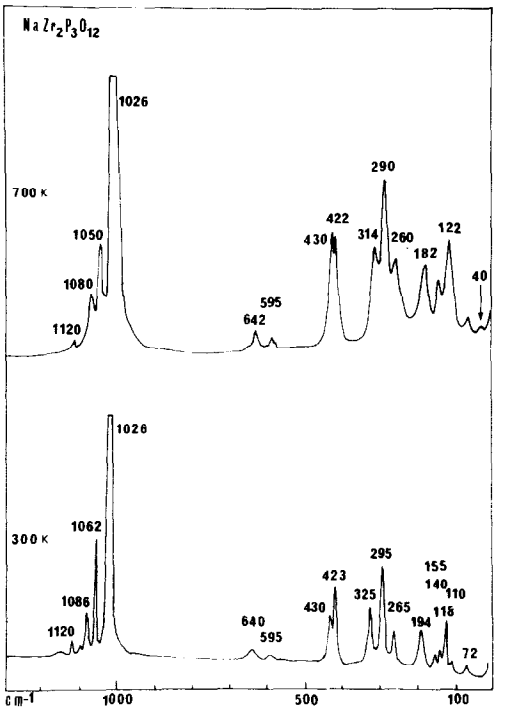

FIG. 6. Raman spectra of $NaZr_2P_3O_{12}$ at 300 and 700 K.

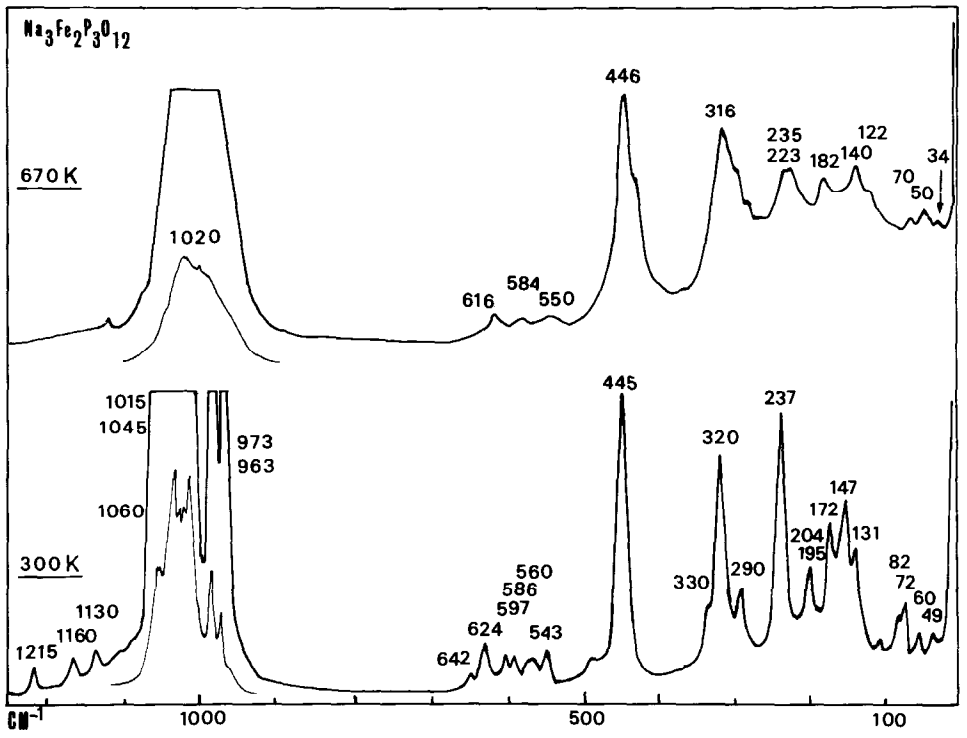

FIG. 7. Raman spectra of $Na_3Fe_2P_3O_{12}$ at 300 and 670 K.

origin of this SSRD is attributed to the partial occupation of the Na(1) and Na(2) sites (rhombohedral description). However, the Raman spectrum recorded for $Na_3Fe_2(PO_4)_3$ at 300K, presented in Fig. 7, is typically a spectrum of a well-ordered network. The Na(1) site is totally filled (*2*). So, the origin of the SSRD is attributed *exclusively to the partial occupation of the Na(1) site*. This is corroborated by the fact that in the disordered $Na_3Cr_2(PO_4)_3$ the occupation factor of Na(1) site is equal to .83 at 300 K.

Evolution with temperature. As shown in Fig. 6 the Raman spectra of the ordered $NaZr_2(PO_4)_3$ does not exhibit significant spectral change when the temperature is increased. Only slight broadening of the Raman components is observed. This indicates that this zirconium phosphate keeps its short-range order even at 700 K, and that the occupation factor of the Na(1) site seems to remain close to unity. This compound does not undergo any phase transition in this temperature range. Nevertheless, in order to take into consideration the existence of a second Na^+ site deduced from NMR measurements on $NaZr_2(PO_4)_3$ (*5*), one could be tempted to relate the presence of a new weak Raman band at 40 cm^{-1} (700 K) with the occupation of such a site. However, the occupation of this site could be very low (less than 10%) in order to induce (through Na(1) site partial occupation) spectroscopically observable disorder.

Figure 7 presents the Raman spectra of $Na_3Fe_2(PO_4)_3$ recorded at 300 and 670 K corresponding respectively to the monoclinic α-phase and the rhombohedral γ-phase (*2*). These spectra illustrate the establishment of the short-range disorder as a function of the

temperature and resulting from the decrease of the Na(1) site occupancy. It has been shown (*8*) that the occupation factor of the Na(1) site in the iron phosphate decreases from 1 at 300 K to 0.91 at 393 K. This confirms that the partial filling of the Na(1) site is a determining factor causing short-range disorder accompanied by Na^+ higher mobility. As for electrons, the repulsion effect considered in the Mott–Hubbard model leads to a nonconducting solid when there is one charge carrier per regular site or on the contrary when there is no hole left. Thus, the presence of extra Na^+ ions creates subminima at Na(2) sites in the lattice potential energy curve as shown in recent calculations (*11*). This can be correlated: (i) with the presence of low-frequency temperature-sensitive bands attributed to the mobile cation motions. That is the case for the Raman doublet at 49–60 cm^{-1} (300 K) observed in the iron compound which softens to 34–50 cm^{-1} at 670 K, indicating a lowering of the local potential barrier (*2*); (ii) with the ionic conductivity which is maximum (*4*) for the intermediate composition of the phosphate solid solutions where the sodium content is around 3. That is also the case of the silicophosphate solid solutions, where the highest conductivity is observed (*1*) for the $Na_3Zr_2Si_2PO_{12}$ composition called Nasicon.

6. Conclusion

The infrared Raman study of two chromium solid solutions belonging to the Nasicon family has allowed the correlation of the spectral evolution of the modes involving PO_4 and LO_6 motions to the crystal field modifications in agreement with the structural studies reported in the literature. The broadening and the number reduction of the Raman components were interpreted in terms of static short-range disorder directly correlated to the partial occupation of the Na(1) site. The broadening of the Raman spectrum can thus be considered as an indication of the existence of vacant Na(1) sites and could be used for characterizing and indicating potential ionic mobility in this family of materials.

The mobile cation modes were identified in the low-frequency region. The far-infrared observed bands at 85 cm^{-1} and around 50 cm^{-1} are attributed to Na^+ motions respectively in the Na(1) and Na(2) sites. In the Raman spectra, the lowest frequency peak, at about 60 cm^{-1} in $Na_2CrZr(PO_4)_3$ and $Na_4CrMg(PO_4)_3$ and at 50 cm^{-1} in $Na_3Cr_2(PO_4)_3$, is attributed to Na^+ motions in the Na(2) site. The lowest value of this mode observed in $Na_3Cr_2(PO_4)_3$ could be associated with a relatively higher mobility of the sodium ions in this compound compared to the other terms of the solid solutions studied here. This is corroborated by the following observations:

—the existence of an important short-range disorder in the best conducting compositions (we have already also observed this in the "true" Nasicon).

—the increase of the mean frequency of the phosphate ions internal modes, indicating an increase in the covalency of the P–O bonds.

References

1. H. Y-P. Hong, *Mater. Res. Bull.* **11,** 173 (1976).
2. M. Barj, *Thesis Etat, Paris XIII* (1987).
3. M. Barj, H. Perthuis, and P. Colomban, *Solid State Ionics* **11,** 157 (1983).
4. C. Delmas, F. Cherkaoui, and P. Hagenmuller, *Mater. Res. Bull.* **21,** 469 (1986).
5. F. Cherkaoui, G. Villeneuve, C. Delmas, and P. Hagenmuller, *J. Solid State Chem.* **65,** 293 (1986).
6. C. Delmas, J. C. Viala, R. Olazcuaga, G. Le Flem, F. Cherkaoui, R. Brochu, and P. Hagenmuller, *Solid State Ionics* **3/4,** 209 (1981).
7. F. D'Yvoire, M. Pintard-Screpel, E. Bretey, and M. De La Rochere, *Solid State Ionics* **9/10,** 851 (1983).
8. M. De La Rochere, F. D'Yvoire, G. Collin, and R. Comes, *Solid State Ionics* **9/10,** 825 (1983).

9. M. BARJ, K. CHHOR, L. ABELLO, C. POMMIER, AND C. DELMAS, *Solid State Ionics* **28/30,** 432 (1988).
10. G. LUCAZEAU, M. BARJ, J. L. SOUBEYROUX, A. J. DIANOUX, AND C. DELMAS, *Solid State Ionics* **18/19,** 959 (1986).
11. J. F. BOCQUET, M. BARJ, G. LUCAZEAU, AND G. MARIOTTO, *Solid State Ionics* **28/30,** 411 (1988).
12. L. O. HAGMAN AND P. KIERKEGAARD, *Acta Chem. Scand.* **22,** 1822 (1968).
13. R. G. SIZOVA, A. A. VORONKOV, N. G. SHUMYATSKAYA, V. V. ILYUKHIM, AND N. V. BELOV, *Sov. Phys. Dokl.* **17,** 618 (1973).
14. L. ABELLO, K. CHHOR, M. BARJ, C. POMMIER, AND C. DELMAS, *J. Mater. Sci.* **24,** 3380 (1989).
15. F. CHERKAOUI, *Thesis Etat, Bordeaux* (1985).
16. K. NAKAMOTO, "Infrared and Raman Spectra of Inorganic and Coordination Compounds," Wiley, New York (1978).
17. M. BARJ, to be submitted for publication.
18. P. TARTE, A. RULMONT, AND C. MERKAERT-ANSAY, *Spectrochim. Acta* **42A,** 1009 (1986).